

University of Texas Rio Grande Valley

ScholarWorks @ UTRGV

Mechanical Engineering Faculty Publications
and Presentations

College of Engineering and Computer Science

2006

The effect of the shear-thickening transition of model colloidal spheres on the sign of N_1 and on the radial pressure profile in torsional shear flows

M. Lee

University of Utah

Mataz Alcoutlabi

The University of Texas Rio Grande Valley, mataz.alcoutlabi@utrgv.edu

J. J. Magda

University of Utah

C. Dibble

The University Of Michigan

M. J. Solomon

The University Of Michigan

Follow this and additional works at: https://scholarworks.utrgv.edu/me_fac

See next page for additional authors



Part of the [Mechanical Engineering Commons](#)

Recommended Citation

Lee, M.; Alcoutlabi, Mataz; Magda, J. J.; Dibble, C.; Solomon, M. J.; Shi, X.; and McKenna, G. B., "The effect of the shear-thickening transition of model colloidal spheres on the sign of N_1 and on the radial pressure profile in torsional shear flows" (2006). *Mechanical Engineering Faculty Publications and Presentations*. 10.

https://scholarworks.utrgv.edu/me_fac/10

This Article is brought to you for free and open access by the College of Engineering and Computer Science at ScholarWorks @ UTRGV. It has been accepted for inclusion in Mechanical Engineering Faculty Publications and Presentations by an authorized administrator of ScholarWorks @ UTRGV. For more information, please contact justin.white@utrgv.edu, william.flores01@utrgv.edu.

Authors

M. Lee, Mataz Alcoutlabi, J. J. Magda, C. Dibble, M. J. Solomon, X. Shi, and G. B. McKenna

The effect of the shear-thickening transition of model colloidal spheres on the sign of N_1 and on the radial pressure profile in torsional shear flows

M. Lee, M. Alcoutlabi, and J. J. Magda^{a)}

*Department of Chemical Engineering, University of Utah,
50 S. Central Campus Drive, Room 3290, Salt Lake City, Utah 84112*

C. Dibble and M. J. Solomon

*Department of Chemical Engineering, University of Michigan,
Ann Arbor, Michigan 48109*

X. Shi and G. B. McKenna

*Department of Chemical Engineering, Texas Tech University,
Lubbock, Texas 79415*

(Received 16 August 2005; final revision received 14 February 2006)

Synopsis

A novel rheometer plate was used to measure radial pressure profiles during cone-and-plate and parallel-plate shearing flows of a concentrated colloidal dispersion of poly(methyl methacrylate) spheres suspended in dioctyl phthalate. There is a long history of using suspensions of this type as a model rheological system. The measured pressure profile can be used to calculate N_1 and N_2 , and also provides a check on the flow field in the rheometer. At shear rates just below onset of shear thickening, our measurements show that N_1 is positive as predicted by Stokesian dynamics simulations of model Brownian hard spheres, but we are unable to determine the sign of N_2 . After the onset of thickening, we find that in both flow geometries the pressure increases sharply with radial position. This is in striking contrast to the pressure profiles ordinarily observed for viscoelastic liquids (with the exception of certain liquid crystal polymers), for which the pressure decreases with radial position. Under these conditions, the apparent values of N_1 and N_2 are both negative with $|N_2| > |N_1|$, as predicted by the Stokesian dynamics simulations. However, the flow in the cone-and-plate rheometer may not be viscometric after the onset of shear thickening. © 2006 The Society of Rheology. [DOI: 10.1122/1.2188567]

I. INTRODUCTION

For model suspensions in Newtonian solvents thought to approximate hard spheres, there is ample experimental evidence that both the first (N_1) and second (N_2) normal stress differences are negative in the high Peclet number regime, with $|N_2| > |N_1|$ [Zarraga *et al.* (2000), Singh and Nott (2003)]. However, experimental measurements of

^{a)}Author to whom correspondence should be addressed; electronic mail: jj.magda@m.cc.utah.edu

the normal stress differences at lower Peclet numbers where Brownian motion is important are lacking [Brady (2000)]. Here, the Peclet number $Pe = 6\pi\eta_s a^3 \dot{\gamma} / (kT)$ is a measure of the importance of shear forces compared to Brownian forces, where $\dot{\gamma}$ is the shear rate, a is the particle radius, and η_s is the solvent viscosity. Values of N_1 and N_2 are important for suspensions, because normal stress differences can drive the migration of particles across streamlines in nonhomogeneous shearing flows [Brady (2000)]. The above-mentioned experimental studies of N_1 and N_2 employed rather large spheres ($a > 20 \mu\text{m}$), hence very large Peclet number flows were unavoidable [$Pe \approx O(10^7)$]. Here we report normal stress measurements on suspensions prepared with much smaller model colloidal spheres ($a = 0.295 \mu\text{m}$), which allowed us to access lower Pe values than previously studied ($65 < Pe < 950$). According to Stokesian dynamics hard sphere simulations, N_1 should be positive when the Peclet number is low enough for Brownian forces to dominate [Foss and Brady (2000)]. With increasing shear rate, the signature of the transition into a hydrodynamics-dominated flow regime is a reversible viscosity shear-thickening transition. Shear thickening is predicted to occur when the hydrodynamic forces become strong enough to push particles very close together into “dynamic particle clusters” [Bossis and Brady (1989); Phung *et al.* (1996); Melrose *et al.* (1996); Foss and Brady (2000)]. The Stokesian dynamics simulations also make the remarkable prediction that N_1 changes sign from positive to negative at the shear-thickening transition [Brady (2000); Foss and Brady (2000)]. The predicted behavior of the viscosity at the shear-thickening transition has been verified (at least qualitatively) in many experimental studies of colloids thought to approximate hard spheres [Mewis *et al.* (1989); D’Haene *et al.* (1993); Frith *et al.* (1996); Bender and Wagner (1996); Lee *et al.* (1999); Mewis and Biebaut (2001); Maranzano and Wagner (2001)]. However, as far as we know, the predicted sign change of N_1 has not yet been verified prior to the current study.

For suspensions of perfectly smooth hard spheres, both N_1 and N_2 should approach zero as $Pe \rightarrow \infty$ [Brady and Morris (1997)]. However, it is probably impossible to prepare perfect hard spheres; real hard spheres inevitably have a small amount of surface roughness and an excluded volume force of short yet finite range [Rampall *et al.* (1997); Foss and Brady (2000)]. If any repulsive force at all is added to the hard sphere potential, no matter how short in range, then both N_1 and N_2 are found in Stokesian dynamics simulations to scale linearly with the shear rate at high Peclet numbers [Brady (2000); Singh and Nott (2000)]. Furthermore, both N_1 and N_2 are predicted to be negative, with N_2 either exceeding or comparable to N_1 in magnitude, depending on whether particle friction is included or not [Sierou and Brady (2002)]. Thus, the Stokesian dynamics simulation predictions are consistent with the available experimental results at high Peclet number.

The colloidal system investigated here contained nearly monodisperse poly(methylmethacrylate) (PMMA) spheres that were coated with a thin steric layer ($\approx 10 \text{ nm}$) of poly(12-hydroxystearic acid), and suspended in the high-boiling organic solvent dioctyl phthalate (DOP). There is a long history of using suspensions of this type as a model rheological system to approximate hard spheres [Ackerson and Pusey (1988); Mewis *et al.* (1989); D’Haene *et al.* (1993); Frith *et al.* (1996); Petekidis *et al.* (2002, 2004)]. However, after we initiated this study, works have appeared in the literature that might lead one to question the validity of the hard sphere approximation as applied to sterically-stabilized PMMA spheres [Yethiraj and van Blaaderen (2003); Krishnamurthy *et al.* (2005)]. Suspensions of sterically stabilized PMMA particles are known to crystallize at rest at a particle volume fraction $\phi \approx 0.495$, in agreement with molecular dynamics simulations of perfectly smooth hard spheres [Campbell and Bartlett (2002)]. However, during flow at the shear-thickening transition, the interparticle spacing within the dynamic par-

ticle clusters can be quite small [Foss and Brady (2000); Maranzano and Wagner (2001)]. In this situation, even a slight departure from the perfect hard sphere potential due to the thin polymer coat or due to a slight surface charge can be important. As a consequence, for sterically stabilized PMMA spheres, the experimental value of the Peclet number for onset of shear thickening is larger than predicted by the Stokesian dynamics simulations ($Pe_c \approx 100$ vs 10) [D'Haene *et al.* (1993); Foss and Brady (2000); Maranzano and Wagner (2001); Krishnamurthy *et al.* (2005)]. Using a two-particle model, Bergenholtz and co-workers have investigated the significance of deviations from the hard sphere model by varying the range of the repulsive force between particles and noting the effects on N_1 , N_2 , and the viscosity at the shear-thickening transition [Bergenholtz *et al.* (2002)]. In this theoretical study, the excluded volume parameter b/a was varied from 1 to infinity, with b defined as the effective radius of a particle in the presence of a repulsive steric layer, and a defined as the radius of a bare hard sphere. Normal stress results presented here will be interpreted using this theory.

In the following sections, we describe measurements of N_1 at shear rates below the onset of shear thickening using oversize rheometer plates, and the use of the measured radial pressure profile to check the nature of the flow field in the rheometer after onset of thickening. There are reasons to suspect that rheometer flows of model hard sphere suspensions may not be well behaved after onset of shear thickening. Both Singh and Nott (2003) and Kolli *et al.* (2002) have reported large time-dependent fluctuations in the measured normal force value. As pointed out by Mewis and Biebaut (2001), if the dynamic particle clusters responsible for shear thickening become comparable in size to the rheometer gap, this will compromise rheological measurements. This was a principal reason for using both parallel-plate and cone-and-plate flow geometries in the current work.

II. MATERIALS AND PARTICLE CHARACTERIZATION

PMMA colloids stabilized with polyhydroxyteric acid (PHSA) dispersed in approximately refractive index matched solvents are a model system for rheological studies [Ackerson and Pusey (1988); Mewis *et al.* (1989); D'Haene *et al.* (1993); Frith *et al.* (1996); Petekidis *et al.* (2002, 2004)]. The PHSA graft layer promotes stability in non-polar organic solvents such as decalin, cyclohexyl bromide (CHB) and DOP and their mixtures. Dispersion in a solvent that approximately matches the refractive index of the PMMA colloids minimizes van der Waals interactions that can yield to gelation and phase separation [Russel *et al.* (1989)]. Here, we prefer to study submicron colloids stably dispersed in DOP because the small size of the particles and the high viscosity of the solvent shift the system Peclet number into the range accessible to the rheological instrumentation.

The synthesis of the PMMA particles sterically stabilized with PHSA proceeds in three steps. First, a modified version of Campbell and Bartlett's method (2002) is used to synthesize the PHSA stabilizer. The PHSA stabilizer is a comb-shaped graft copolymer with PHSA fingers protruding from a methyl methacrylate and glycidyl methacrylate backbone [Pathmamanoharan *et al.* (1997)]. Second, the stabilizer is used in the dispersion polymerization of methyl methacrylate to form the submicron colloidal particles as per Antl *et al.* (1986). Third, the PHSA stabilizer is covalently locked onto the particles to ensure their long-term stability. The following modifications from the published procedures were used in this study: (1) The reactants in the dispersion polymerization were scaled to a lower monomer concentration of 34% by weight based on the relationship [Antl *et al.* (1986)] between monomer concentration and particle size to produce particles

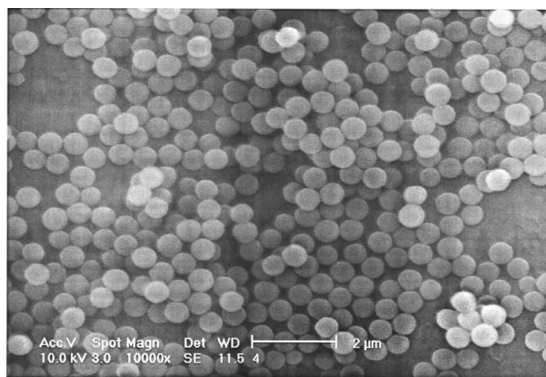


FIG. 1. SEM micrograph of PMMA model colloid without solvent.

smaller than one micron. (2) No fluorescent dye was incorporated into the particles as in Campbell and Bartlett (2002), because only rheological measurements were performed. (3) The amount of PHSA stabilizer incorporated was increased to 12% by weight to prevent aggregation during the synthesis.

The synthesized colloids were cleaned, dried, and imaged by scanning electron microscopy (SEM). Analysis of the resulting images characterizes the size and polydispersity of the particles. Figure 1 contains an SEM micrograph of the PMMA model colloid (note that there is no suspending solvent in this case). The colloids are observed to be monodisperse in size and shape. From image analysis, we determine that the colloidal spheres have a diameter of 590 nm. The standard deviation of particle diameter distribution is 3.6% relative to the mean size. Particles were suspended in dioctyl phthalate (DOP, Sigma Aldrich) by vortex mixing. Stability of the suspension was ascertained by means of direct microscopic visualization of analogously prepared fluorescent suspensions (data not shown). We note that the effective diameter of the colloids in DOP may differ slightly from the SEM result due to particle swelling and repulsive interactions [Yethiraj and van Blaaderen (2003); Royall *et al.* (2003)].

III. RHEOMETRY

Cone-and-plate rheology measurements were performed at the University of Utah at room temperature on the shear-rate-controlled Weissenberg R-17 rheometer. Three different cones were used, two with radius R equal 1.25 cm (cone angles: 0.020 rad and 0.038 rad), and one with radius 3.7 cm (cone angle 0.065 rad). The two smaller diameter cones were used with a novel rheometer plate (RheoSense, Inc., San Ramon, CA) containing eight miniature pressure sensors, four on each side of the plate at locations symmetric about the plate center point. The larger diameter cone was used with a conventional rheometer plate without pressure sensors. On the pressure sensor plate, each sensor measures the local value of the “pressure”, or more precisely, the vertical diagonal component of the total stress tensor (Π_{22}). For a steady cone-and-plate shearing flow that is viscometric and of uniform shear rate, Π_{22} is expected to have the following dependence on radial position r [Bird *et al.* (1987)]:

$$-\Pi_{22} - P_0 = -(N_1 + 2N_2)\ln(r/R) - N_2, \quad (1)$$

where P_0 is atmospheric pressure. According to Eq. (1), a plot of $-\Pi_{22} - P_0$ versus $\ln(r/R)$ should yield a straight line, in which case the slope of this line and its intercept

($r \rightarrow R$) can be used to calculate both N_1 and N_2 . Equation (1) is derived assuming that the cone-and-plate flow is viscometric and of uniform shear rate, and that there is no jump in the value of the total stress component Π_{33} at the sample/air interface [Bird *et al.* (1987)]. If the base flow field is disturbed, perhaps because of “particle jamming” that arises from the formation of large colloid particle clusters [Mewis and Biebaut (2001); Maranzano and Wagner (2001)], then there is little reason to expect that Π_{22} will have a logarithmic dependence on radial position r . Thus measurement of the radial pressure profile $\Pi_{22}(r)$ provides an indirect check on the stability of the flow field in the rheometer. Cone-and-plate measurements with a similar monolithic pressure sensor plate have been shown to yield accurate values of N_1 and N_2 for a moderately elastic reference polymer solution from NIST [Baek and Magda (2003)]. Unfortunately, similar measurements on the colloid sample were not possible at shear rates below the onset of shear thickening due to low normal stress levels.

At shear rates below the onset of viscosity shear thickening, we found it necessary to measure N_1 by switching to the larger diameter cone-and-plate fixture ($R=3.74$ cm) and using the very sensitive normal force spring of the Weissenberg R-17 rheometer (spring constant $K \approx 10\,000$ N/m). With this configuration, the value of N_1 can usually be measured with an accuracy of approximately 0.1 Pa [Lee (2004)]. In these experiments, the radial pressure profile was not measured, and thus N_2 could not be calculated.

Parallel-plate rheology measurements were performed at Texas Tech University at 25 °C on a shear-rate-controlled ARES rheometer (TA Instruments). This rheometer has been modified as discussed in a previous study in order to eliminate thermal heating due to transducer feedback loops [Niemi *et al.* (1996)]—the torque and normal force rebalance transducers from the rheometer manufacturer were replaced with semiconductor strain gauges [Hutcheson *et al.* (2004)]. The radius of the parallel plate fixture used was 1.25 cm, and the gap was varied between 0.8 mm and 1.1 mm. One of the parallel plates was a monolithic pressure sensor plate similar to the one used at Utah. This plate was also manufactured by RheoSense, Inc., and was used to measure the radial pressure profile $\Pi_{22}(r)$. Thus, the total vertical thrust exerted by the colloid in the parallel-plate rheometer was measured simultaneously using both the pressure sensor plate and the strain gauge transducer. However, the strain gauge transducer on the ARES rheometer at Texas Tech University was designed for polymer melts and is less sensitive than the normal force spring transducer on the Weissenberg rheometer. The sensitivity of the parallel plate normal thrust measurements with the strain gauge transducer was approximately 100 Pa with the flow geometry used. An expression for the radial pressure profile in the parallel-plate rheometer analogous to Eq. (1) has been derived assuming a viscometric flow field in which the shear rate $\dot{\gamma}$ increases linearly with radial position r [Adams and Lodge (1964)]:

$$r(d\Pi_{22}/dr) = d\Pi_{22}/d(\ln r) = N_1 + N_2 + \dot{\gamma}dN_2/d\dot{\gamma}. \quad (2)$$

As already noted, for ideal cone-and-plate flow, the slope of the radial pressure profile is constant on a logarithmic plot ($d\Pi_{22}/d(\ln r) = \text{constant}$). According to Eq. (2), this is not expected to be the case for parallel-plate flow, because N_1 and N_2 depend on $\dot{\gamma}$ which in turn increases with radial coordinate r . Hence, the parallel-plate geometry is poorly suited for determining the normal stress differences from the measured pressure profile. Nonetheless, it has a gap that is independent of r , which may be advantageous should large colloid particle clusters form during flow. By contrast, in the cone-and-plate geometry, the rheometer gap varies with r and is only about 50 μm near the center of the plate.

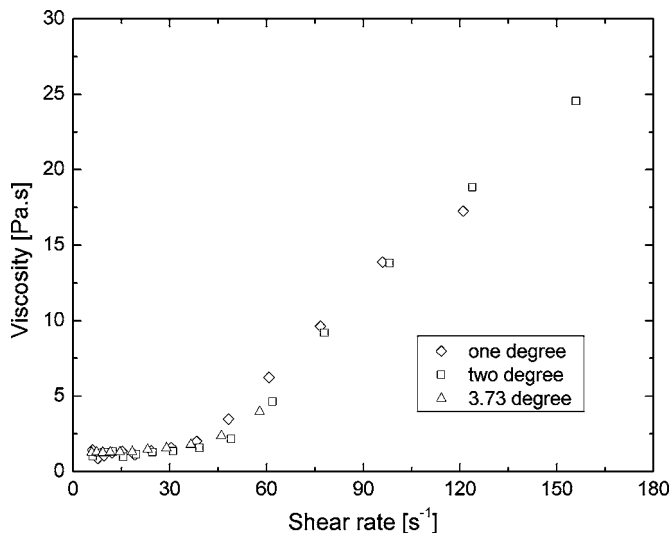


FIG. 2. Viscosity shear-thickening transition of PMMA model colloidal dispersion measured with various cone-plate geometries at the cone angles given in the legend. Cone radius was 3.7 cm for the least shallow cone and 1.25 cm for the other two cones.

IV. RESULTS

A. Viscosity shear-thickening

A concentrated suspension of the colloidal particles in DOP with a volume fraction ϕ of 0.47 (based on the diameter value inferred from the micrograph) exhibits a substantial though continuous shear-thickening transition, as measured at room temperature with three different cone-plate fixtures (Fig. 2). This transition is reversible, i.e., no hysteresis was observed in the measurements of the viscosity versus shear rate. The critical shear rate for onset of thickening is approximately $25 s^{-1}$, and the viscosity results measured with three different cone angles are in good agreement up to a shear rate of about $100 s^{-1}$. It is common rheological practice to vary the cone angle or gap in order to test for the presence of secondary flows or wall slip, yet no evidence of these flow irregularities can be discerned from the viscosity measurements alone. The observed shear-thickening behavior is roughly consistent with results reported earlier at $\phi=0.47$ for colloidal systems that should have essentially the same interparticle potential, namely systems of PMMA spheres stabilized by PHSA and dispersed in DOP [D’Haene *et al.* (1993); Frith *et al.* (1996)]. D’Haene *et al.* (1993) also made simultaneous flow dichroism measurements and were able to show that the onset of thickening was attributable to the formation of dynamic particle clusters. At higher particle volume fractions ($\phi > 0.56$) in the same PMMA/DOP colloidal system, D’Haene *et al.* observed discontinuous viscosity shear thickening with a shear-rate-controlled rheometer [D’Haene *et al.* (1993)]. One would expect a slight shear-thinning behavior at shear rates below the onset of thickening [de Kruif *et al.* (1985), Frith *et al.* (1996)], but our measurements were too noisy to confirm this. Nonetheless, following Frith *et al.* (1996), we denote the minimum viscosity value measured just before onset of thickening divided by the solvent viscosity as the “high” (really, the intermediate) shear plateau relative viscosity $\eta_{r\infty}$. Using experimental results for sterically stabilized PMMA colloids in various solvents including DOP, Frith *et al.* (1996) constructed a universal curve relating $\eta_{r\infty}$ to the particle volume fraction corrected for solvent effects on the poly(12-hydroxystearic acid) steric layer. Surprisingly, in order

to obtain this universal curve, it was necessary to assume that the steric layer collapses in DOP [Frith *et al.* (1996)]. Using the data of Fig. 2 ($\eta_{r\infty} \approx 20$) and the universal curve of Frith *et al.* (1996), we estimate a *corrected* particle volume fraction for our suspension of 0.50. The particle volume fraction is 0.47 for the same suspension as calculated using the particle diameter value inferred from the SEM micrograph (Fig. 1) and the pure densities of PMMA and DOP. The discrepancy can be attributed to the volume occupied by the steric layer, or perhaps to a slight electrostatic repulsion between particles. The corrected particle radius a is thus $(295 \text{ nm})(0.50/0.47)^{1/3} \approx 300 \text{ nm}$, which is the value used to calculate Peclet numbers ($\text{Pe} = 6\pi\eta_s a^3 \dot{\gamma}/kT$) throughout this paper. The value of the critical Peclet number Pe_c at the shear-thickening transition in Fig. 2 is $\text{Pe}_c \approx 130$, and the critical value of the shear stress is approximately 30 Pa. Both of these critical values are in good agreement with previous experimental results for PMMA colloids stabilized by PHSA [Frith *et al.* (1996)], but are an order of magnitude larger than the values predicted for smooth hard spheres without steric layers [Krishnamurthy *et al.* (2005)]. Krishnamurthy and co-workers have recently published a micromechanical model that shows that this discrepancy is a consequence of the PHSA steric layer and its effect on particle cluster formation, and that quantitatively predicts the critical shear stress value for onset of thickening [Krishnamurthy *et al.* (2005)].

B. N_1 values

Despite the shift in the onset of viscosity shear thickening to higher Peclet numbers, we assume that the theoretical prediction of a sign change in N_1 occurring at or near the thickening transition still applies [Foss and Brady (2000); Bergenholtz *et al.* (2002)]. In order to test this prediction, we investigate N_1 values for the same colloidal dispersion for which viscosity values are given in Fig. 2 over the same shear rate range. The time-dependent behavior of N_1 for this dispersion during start-up and relaxation of steady cone-plate shear flow is shown in Figs. 3(a) and 3(b) at shear rates below the shear-thickening transition. At a shear rate of 10 s^{-1} ($\text{Pe}=65$) that is well below the thickening transition at 25 s^{-1} , the steady value of N_1 is small but clearly positive, as measured with respect to both the initial and final normal force baselines [Fig. 3(a)]. This is also observed to be true in Fig. 3(b) at a slightly higher shear rate that is still below the shear-thickening transition, but in this case an overshoot is observed for N_1 during the approach to steady state. From Fig. 3, it is immediately apparent why N_1 has rarely if ever been measured before for model colloids thought to approximate hard spheres below the onset of shear thickening: N_1 has a magnitude of only 0.5–1.0 Pa. We were able to measure such small N_1 values only because we used oversize rheometer plates ($R = 3.74 \text{ cm}$), and because we used the highly sensitive normal force spring of the Weissenberg R-17 rheometer. However, N_1 values of this magnitude are consistent with theory, which predicts N_1 to be of order $\eta_s \dot{\gamma}$ ($\eta_s \approx 0.06 \text{ Pa s}$) for shear rates below onset of thickening [Brady (2000)]. When the shear rate is increased to a value just above the onset of viscosity shear thickening, the positive N_1 value jumps in magnitude by a factor of about 100 (Fig. 4). This observation is consistent with an earlier study of PMMA/DOP colloidal dispersions [D'Haene *et al.* (1993)] in which the normal stress levels were reported to exceed the limit of the transducer at shear rates above the onset of shear thickening, and to be too small to detect at lower shear rates. Thus, at shear rates above the onset of shear thickening, we were able to switch to a smaller radius cone-and-plate fixture ($R = 1.25 \text{ cm}$) and simultaneously measure the vertical forces exerted during flow using the Weissenberg normal force spring and the novel pressure sensor plate. The apparent steady-state value of N_1 as measured with the Weissenberg normal force spring

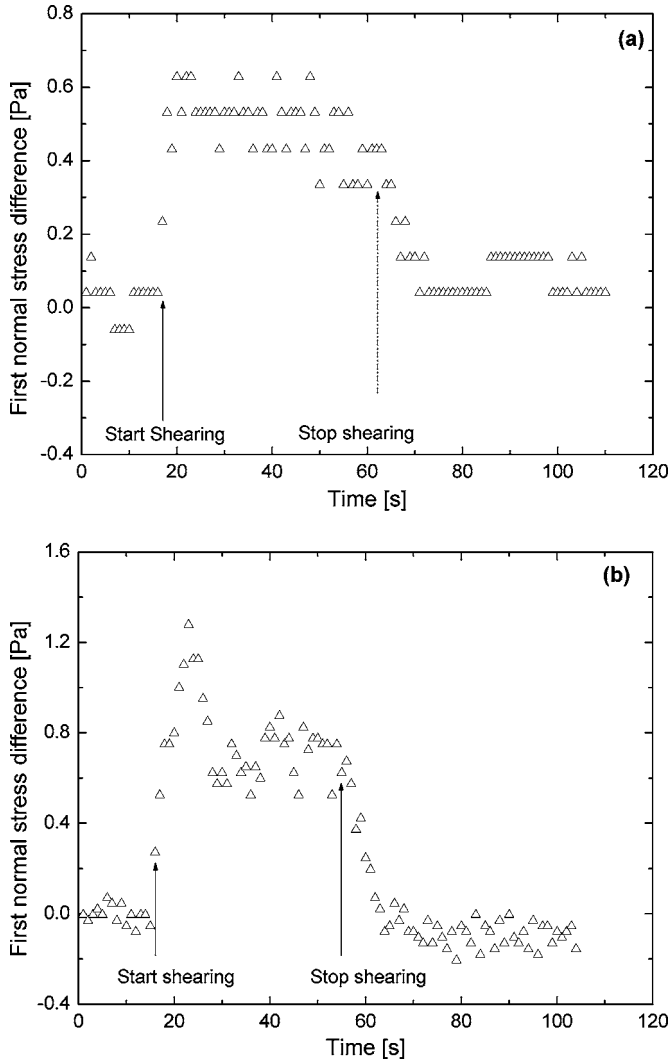


FIG. 3. Startup behavior of N_1 for PMMA model colloidal dispersion at the following shear rates below the shear-thickening transition: (a) 10 s^{-1} , $Pe = 65$, and (b) 13 s^{-1} , $Pe = 82$. Cone radius was 3.74 cm and cone angle was 0.065 rad.

is plotted against shear rate in Fig. 4. Comparison is made between N_1 values measured with the two smaller diameter cones having different cone angles [Fig. 4(a) versus Fig. 4(b)]. The larger diameter cone-plate fixture used at lower shear rates could not be used after onset of shear thickening due to occurrence of sample edge fracture [Larson (1992)], which may be a consequence of highly negative N_2 values [Tanner and Keentok (1983); Lee *et al.* (1992); Huilgol and Phan-Thien (1997); Zarraga *et al.* (2000)]. In Fig. 4, there is a substantial variation in N_1 values measured with different samples and with different cone angles, in striking contrast to the viscosity results for the same suspension (Fig. 2). This large uncertainty in the values of N_1 for the model colloid above onset of shear thickening (Fig. 4) cannot be attributed to inaccuracies in the measurement system. For example, when the same normal force spring and the same cone-and-plate fixture were used to measure N_1 values for a polydimethylsiloxane melt, the sample-to-sample varia-

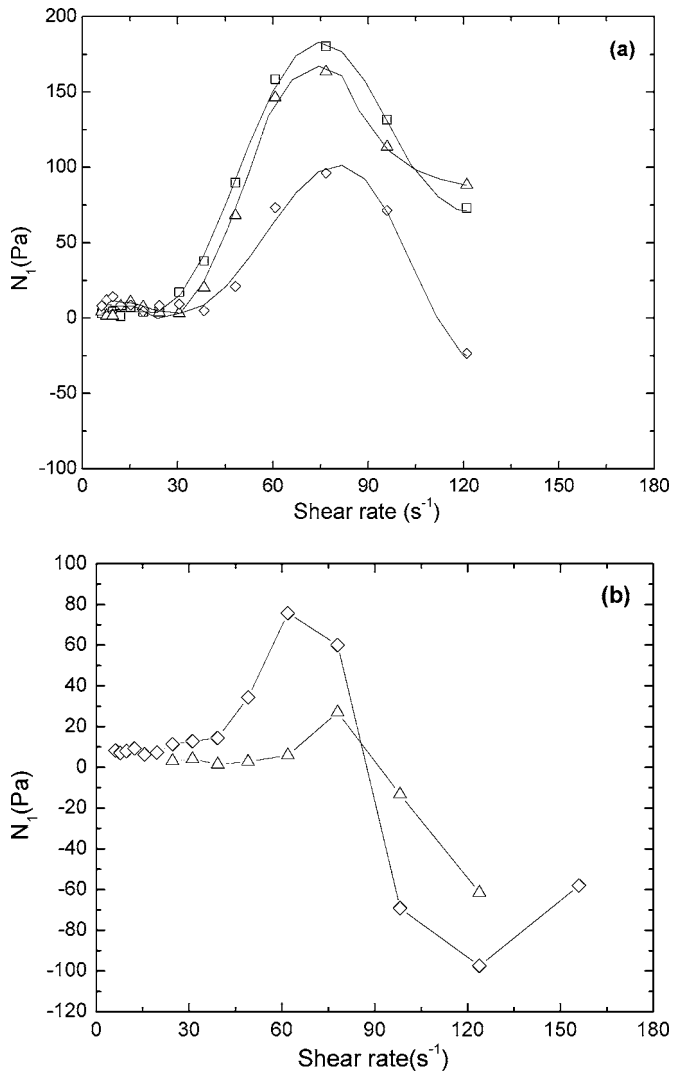


FIG. 4. Apparent steady-state value of N_1 vs shear rate measured for (a) three different samples of model colloidal dispersion using cone of radius 1.25 cm and cone angle of 0.020 rad and (b) two different samples of model colloidal dispersion using cone of radius 1.25 cm and cone angle of 0.038 rad. Onset of viscosity shear thickening occurred at a shear rate $\approx 25 s^{-1}$.

tion in N_1 values was only of order 3 Pa [Lee (2004)]. By contrast, in Fig. 4, the measurement-to-measurement variation in N_1 values for a given sample was of order 25 Pa. Thus, we attribute the much larger variations in N_1 values measured for the colloid to the presence of a flow disturbance, or perhaps to the extreme sensitivity of colloidal systems to small-scale surface interactions [Foss and Brady (2000)]. Nonetheless, despite the large sample-to-sample fluctuations, all results in Fig. 4 are consistent with the same basic shape for the N_1 flow curve, with a positive relative maximum occurring *after* the onset of viscosity shear thickening, followed by negative N_1 values at higher shear rates. At the shear rate of the maximum in N_1 , the change in rheometer gap due to transducer spring compliance is of order $0.5 \mu m$, which should be negligible. Thus, N_1 does appear to exhibit a change in sign from positive to negative as predicted by hard sphere simu-

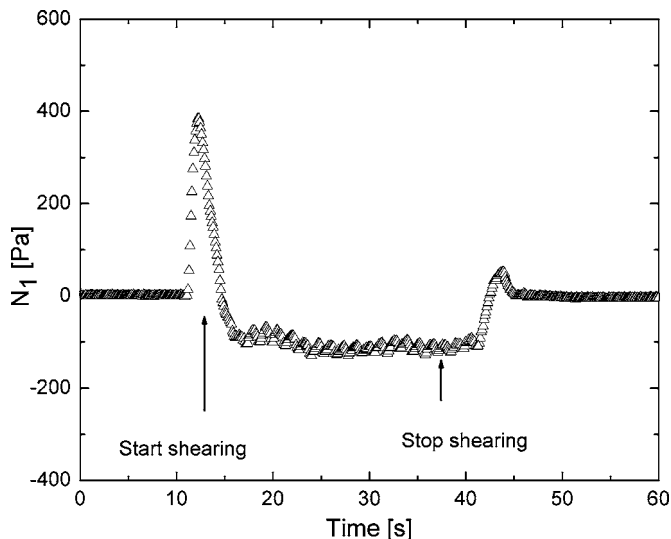


FIG. 5. Startup behavior of N_1 approximately 30 s after flow in the opposite direction was stopped for PMMA model dispersion at a shear rate (124 s^{-1} , $Pe \approx 743$) that is above the shear-thickening transition. Measurements were made using cone of radius 1.25 cm and cone angle of 0.038 rad on the same sample giving the N_1 values represented with diamonds in Fig. 4(b).

lations [Foss and Brady (2000)], but surprisingly the sign change occurs at a shear rate well above the start of the shear-thickening transition. This may possibly be attributed to the presence of the extra repulsive interparticle force of finite range associated with the polymer steric layer, as analyzed theoretically in the paper by Bergenholtz *et al.* (2002). According to Fig. 13 of Bergenholtz *et al.* (2002), when the excluded value parameter b/a is increased from its hard sphere value 1.0 to a value between 1.01 and 1.1, the value of the critical Peclet number at which N_1 changes sign increases by a factor of about 5. Further evidence that b/a exceeds 1.0 for our model colloid system is provided by the large magnitude of measured N_2 values (see next section).

Figure 5 shows the startup behavior of N_1 at a relatively high Peclet number value ($Pe \approx 743$) that was close to the maximum that could be studied without occurrence of sample edge fracture. The results in Fig. 5 clearly show that the steady-state value of N_1 is negative with respect to both the initial and final baselines, and that steady state is achieved within 20 s after initiating shear flow. This is a typical transient time for all the shear rates studied on the Weissenberg rheometer. The time dependence of N_1 in Fig. 5 is quite peculiar: N_1 exhibits a positive overshoot and then approaches a negative steady-state value. This behavior is quite similar to the startup behavior measured for non-Brownian hard sphere suspensions using parallel-plate geometries by Kolli *et al.* (2002) and Narumi *et al.* (2002). These authors attributed this startling transient behavior to the presence of a shear-induced anisotropic suspension structure that undergoes a transition upon flow reversal to its mirror image.

C. Cone-plate pressure profiles and N_2 values

Equation (1) for the radial pressure profile is derived assuming that the flow in the cone-and-plate rheometer is viscometric and of uniform shear rate. These same assumptions are used to derive the equations relating the viscosity to the measured torque on the

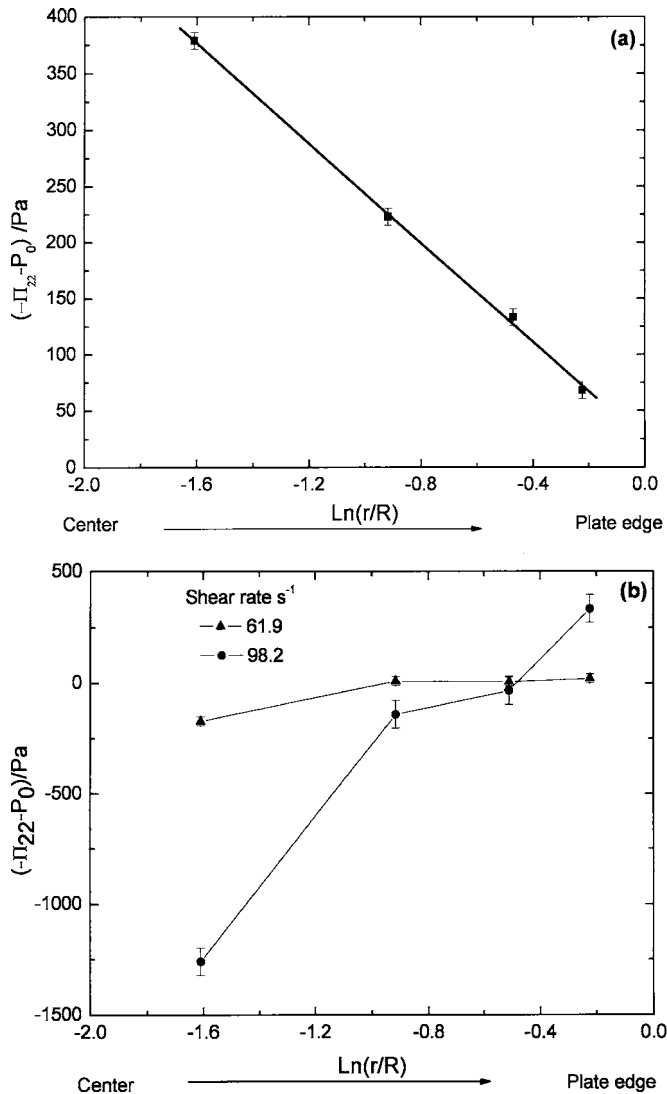


FIG. 6. Time-averaged radial pressure profiles measured during cone-and-plate shearing flows with cone radius 1.25 cm and cone angle 0.038 rad for (a) standard viscoelastic polymer solution from NIST (SRM 1490) at shear rate 4.9 s^{-1} ; average of four measurements with one sample, and (b) PMMA model colloidal dispersion at shear rates shown in legend; average of six measurements with one sample, the same sample giving the N_1 values calculated from total thrust measurements indicated by Δ in Fig. 4(b). Error bars correspond to a confidence interval of 66.7%.

cone, and N_1 to the measured vertical thrust [Bird *et al.* (1987)]. Thus, if measurements show that Eq. (1) is violated, one must conclude that the apparent values of the viscosity and N_1 are also suspect.

Figure 6(a) shows that the radial pressure profile measured with the novel pressure sensor plate for a reference polymer solution from NIST (SRM 1490) does obey Eq. (1). The ordinate is $-\Pi_{22} - P_0$, where P_0 is atmospheric pressure and Π_{22} is the total normal stress component in the velocity gradient direction ($\Pi_{22} > 0$ for a tensile stress by convention). As predicted by Eq. (1), $-\Pi_{22} - P_0$ is a linear function of radial position r in a

logarithmic plot. The slope of this line, which is equal to $-(N_1 + 2N_2)$ according to Eq. (1), is negative. This is as expected, since for most polymers $N_1 > 0$, $N_2 < 0$, and $-N_2 < 0.5N_1$ [Bird *et al.* (1987)]. Furthermore, the measured values of $-\Pi_{22} - P_0$ in Fig. 6(a) are positive; this means that at each radial position, the polymer solution exerts a force per unit area on the plate during flow that exceeds atmospheric pressure. In Fig. 6(a), this force is greater near the center of the plate than at the rim. This is typical behavior for viscoelastic liquids [Adams and Lodge (1964); Bird *et al.* (1987); Magda and Baek (1994); Baek and Magda (2003)]. An exception is liquid crystalline solutions of rodlike polymers that have $N_1 < 0$ [Magda *et al.* (1991)].

By contrast, consider radial pressure profiles measured for the PMMA colloidal dispersion with the same modified cone-and-plate fixture [Fig. 6(b)]. At shear rates below the onset of viscosity shear thickening, $-\Pi_{22} - P_0$ is too small to measure. This is as expected from Eq. (1), since both N_1 and N_2 are believed to be small in magnitude. Figure 6(b) shows the radial pressure profile [$-\Pi_{22} - P_0$ versus $\ln(r/R)$] as measured at two different shear rates (61.9 s^{-1} and 98.2 s^{-1}), both above the onset of shear thickening. For both shear rates, the apparent value of N_1 was measured simultaneously using the normal force spring [indicated with Δ in Fig. 4(b)]. The error bars on the measured pressure profile are much larger in Fig. 6(b) than in Fig. 6(a), even though the measurement system was the same, which we suspect is due to the presence of a flow disturbance in the colloid. Nonetheless, $-\Pi_{22} - P_0$ clearly *increases* with radial position for the colloidal dispersion at both shear rates, in striking contrast to the behavior observed for the polymer solution from NIST in Fig. 6(a) and for most other viscoelastic liquids that we have studied [Magda and Baek (1994); Baek and Magda (2003)]. Furthermore, at the higher shear rate value, the measured value of $-\Pi_{22} - P_0$ is *negative* over most locations on the plate, which is consistent with the negative value for N_1 at this shear rate in Fig. 4(b). At the highest shear rate studied, 123.8 s^{-1} [not shown in Fig. 6(b)], the positive slope observed for the pressure profile was even more dramatic, increasing from -2400 Pa at the location of the innermost sensor to $+600 \text{ Pa}$ at the location of the outermost sensor. Corrections to the pressure for inertia [Turian (1972)] are quite small under these conditions (less than 1 Pa). These aspects of the behavior of the colloidal dispersion in the cone-and-plate rheometer are highly unusual, but they are entirely consistent with Stokesian dynamics simulations [Foss and Brady (2000)]. The simulations predict that the combination $N_1 + 2N_2$ is negative for hard sphere colloids after onset of shear thickening. If $N_1 + 2N_2$ is negative, then Eq. (1) predicts a positive slope for the cone-and-plate radial pressure profile, which is precisely what is observed in Fig. 6(b). However, the steepness of the positive slope at the higher shear rate in Fig. 6(b) is greater than can be explained using the magnitude of N_1 alone; the negative value of N_2 must also be considered. According to Eq. (1), N_2 values can be obtained by extrapolating the measured pressure profiles to the rim of the rheometer. Estimates of N_2 so obtained are given in Table I. The results in Table I, in combination with the results in Fig. 4(b) for the same sample, show that at the higher shear rates both N_1 and N_2 are negative, and that the magnitude of N_2 exceeds that of N_1 . The latter result may be an additional consequence of the finite range of the repulsive interparticle force associated with the polymer steric layer on the colloid particles. According to the two-particle model of Bergenholtz *et al.* (2002), the high Peclet number ratio of N_2/N_1 is increased by an increase in the excluded volume parameter b/a .

However, the normal stress measurements above the onset of shear thickening are only considered to provide qualitative trends, because the measured pressure profiles in the cone-and-plate rheometer are not linear in Fig. 6(b) as they should be according to Eq. (1). The slope of the pressure profile in Fig. 6(b) appears to be getting steeper at radial

TABLE I. Apparent values of second normal stress difference vs shear rate obtained with a single sample of the model colloidal dispersion [indicated with Δ in Fig. 4(b)]; average of six measurements at each shear rate using cone of radius 1.25 cm and cone angle of 0.038.

Shear rate (s^{-1})	N_2 (Pa) ^a
61.9	-20 ± 40
78	-200 ± 40
98.2	-400 ± 110
123.8	-800 ± 210

^aCalculated using Eq. (1) by extrapolating to the rim the pressure measured at the three outermost sensor locations; innermost sensor signal not used due to possible flow disturbance at $r=2.5$ mm because of small gap or proximity to truncated area of cone.

positions approaching the tip of the cone ($r \rightarrow 0$), which makes it difficult to calculate reliable N_1 values from the pressure profile due to large extrapolation uncertainties. Given the large error bars in Fig. 6(b), it is possible that the true pressure profile is linear if we exclude the innermost sensor reading, but then the question arises: Why are the errors bars so much larger in Fig. 6(b) than in Fig. 6(a)? The accuracy and precision of the pressure sensors on the sensor plate from RheoSense, Inc. is better than 10 Pa, but this value of course does not reflect any possible effects of cone-and-plate flow disturbances. For repeated shear experiments, the standard deviation of the pressure sensor measurements was 7.5 Pa for the standard polymer solution of Fig. 6(a), 20 Pa for the model colloid of Fig. 6(b) at shear rate $62 s^{-1}$, and 62.5 Pa for the model colloid of Fig. 6(b) at $98 s^{-1}$. Given the larger standard deviations for both local pressure measurements and for total thrust measurements (Fig. 4), it seems likely that there is a disturbance of some kind to the base flow of the model colloid in the cone-plate rheometer. Thus, at shear rates above the onset of shear thickening, the flow of the model colloid violates at least one of the assumptions ordinarily assumed to be valid for cone-and-plate shearing flows. The explanation for this is not obvious. Chow and co-workers (1994) have shown experimentally that non-Brownian spheres migrate during sustained shearing flows in Couette rheometers, and that no migration occurs in parallel-plate rheometers. However, the effective diffusion coefficient for this migration is thought to scale as the square of the particle radius, and our particle radius value was at least two orders of magnitude smaller than that of particles studied by Chow *et al.* (1994). Thus, our experiments were probably too short (≈ 30 s) to produce significant particle migration. Furthermore, the viscosity value measured by the cone-and-plate rheometer was not observed to decay or increase with shearing time as would be expected to be the case if particle migration did occur. An alternative hypothesis is that the flow was disturbed by the formation of dynamic particle clusters comparable in size to the rheometer gap near the tip of cone, where the gap is only $56 \mu\text{m}$, as compared to 0.5 mm at the rheometer rim. Such a phenomenon occurring near the cone tip may have little effect on the measured viscosity value (Fig. 2), because torque measurements are dominated by contributions from sample at the larger radial positions. However, since the novel pressure sensor plate has a sensor located only 2.5 mm from the geometric center of the plate, the pressure profile measurements should be more sensitive to flow disturbances near the cone tip than viscosity measurements.

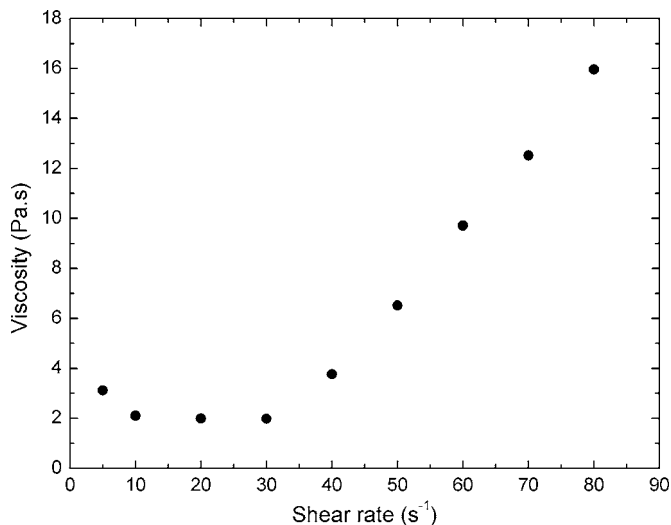


FIG. 7. Apparent viscosity of PMMA model colloidal dispersion vs rim shear rate as measured with a parallel-plate fixture of radius 1.25 cm and with gap 0.86 mm in a shear-rate-sweep experiment.

D. Parallel-plate pressure profiles

One possible reason that the cone-plate pressure profile was found to violate Eq. (1) is particle-jamming, i.e., formation of dynamic particle clusters comparable in size to the rheometer gap [Mewis and Biebaut (2001)]. In order to test for this possibility, we measured the radial pressure profile for the same colloidal suspension during parallel-plate shearing. In the cone-and-plate fixture, the gap was only $56 \mu\text{m}$ near the tip of the cone, which is large compared to an individual particle, but perhaps not large compared to a particle cluster. In the parallel-plate rheometer, the gap chosen was much larger, of order 1 mm. For a model suspension containing much larger spheres ($a > 20 \mu\text{m}$) than studied here, Zarraga and co-workers (2000) have shown that a parallel-plate gap of 1 mm is sufficiently large to avoid wall slip effects on the viscosity. Unfortunately, the larger gap also increased the likelihood of sample ejection from the rheometer during prolonged shearing at high shear rates. Therefore, parallel-plate measurements were made on the ARES rheometer in shear rate sweep experiments. That is, the rim shear rate imposed on the sample was systematically increased from 10 s^{-1} to 100 s^{-1} in increments of 10 s^{-1} , with a shearing time of 60 s at each value of the shear rate. According to the cone-and-plate results already presented (Fig. 5), 60 s is more than enough time to measure the steady shear properties of the suspension, but is not so long as to result in sample ejection. Furthermore, measurements of the time-dependent local pressure using the pressure sensor plate confirmed that steady state was achieved at each shear rate within 60 s. Figure 7 shows the apparent viscosity value of the colloidal dispersion as measured in a shear rate sweep experiment. The apparent viscosity value begins to thicken at a rim shear rate value of about 30 s^{-1} , in good agreement with the thickening onset observed with the cone-and-plate fixture (Fig. 2). The radial pressure profile in the parallel-plate fixture should be described by Eq. (2), provided that the flow in the rheometer is visco-metric, and provided that the shear rate increases linearly with radial position. Figure 8 shows the radial pressure profile [$-\Pi_{22} - P_0$ versus $\ln(r/R)$] measured for the reference viscoelastic polymer solution from NIST (SRM1490) in a shear rate sweep experiment. As is the case with cone-and-plate measurements on the same fluid [Fig. 6(a)], the

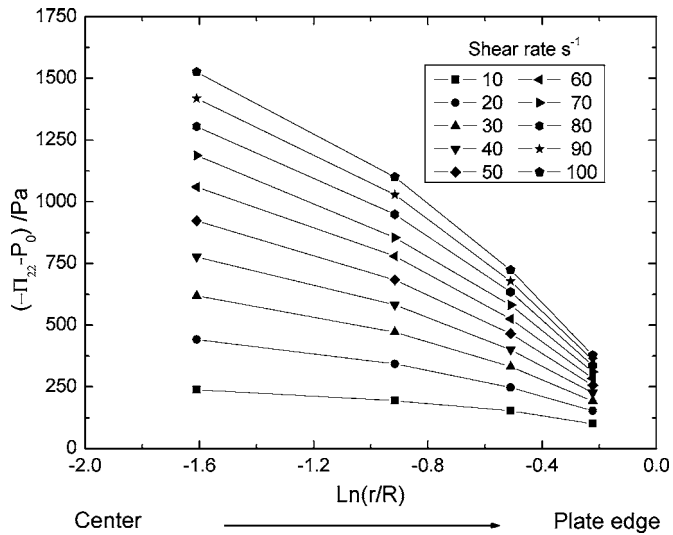


FIG. 8. Time-averaged radial pressure profiles measured during shear-rate-sweep experiments using parallel plate fixtures at the rim shear rates given in the legend for a standard viscoelastic polymer solution from NIST (SRM 1490). The plate radius was 1.25 cm and the gap between the plates was 1.03 mm.

measured value of $-\Pi_{22} - P_0$ is found to be positive, and to decrease with increasing radial position. One difference is that the parallel-plate pressure profile is concave down in a logarithmic plot (Fig. 8). Equation (2) can be used to show that this should be the case for the reference polymer solution. For this polymer solution, $-N_2$ is only $0.1N_1$ [Baek and Magda (2003)], thus it is reasonable to drop the last term in Eq. (2). In this case, Eq. (2) predicts that the slope of the pressure profile at given radial position is approximately equal to $-N_1 - N_2 = -0.9N_1$. Since N_1 is positive and increases with radial position due to increasing shear rate, the slope of the pressure profile should increase in magnitude near the rheometer rim. Hence, the pressure profile in Fig. 8 is concave down.

Figures 9(a) and 9(b) show radial pressure profiles measured for two different samples of the model colloidal dispersion in parallel plate shear rate sweep experiments. During these experiments, the total vertical thrust was also measured when possible using the strain gauge transducer of the modified ARES rheometer. The rim shear rate range covered in the shear rate sweep experiments was $10 - 100 \text{ s}^{-1}$. However, the time-dependent local pressure measurements showed evidence of sample ejection from the rheometer at shear rates above 90 s^{-1} , and the measured radial pressure profile was essentially flat at a value near atmospheric pressure for rim shear rates below the onset of viscosity shear thickening at $\approx 30 \text{ s}^{-1}$. This latter result is unsurprising, given that the cone-and-plate results already presented show that N_1 and N_2 are both small in magnitude below onset of shear thickening. At rim shear rates between these two limits, the measured value of $-\Pi_{22} - P_0$ shown in Fig. 9 is negative and increases with increasing radial position, similar to the trends observed for the same model colloid in the cone-and-plate rheometer [Fig. 6(b)]. Thus, these unusual features are not an artifact of particle jamming near the tip of the cone. The total vertical force measured simultaneously with the strain gauge transducer was positive at each value of the rim shear rate, at least for shear rates above onset of thickening where it was sufficiently large to measure. The radial pressure profile for the colloid sample in Fig. 9 is concave up, and the slope increases dramatically near the rheometer rim. We offer the following hypothesis for the origin of this peculiar shape

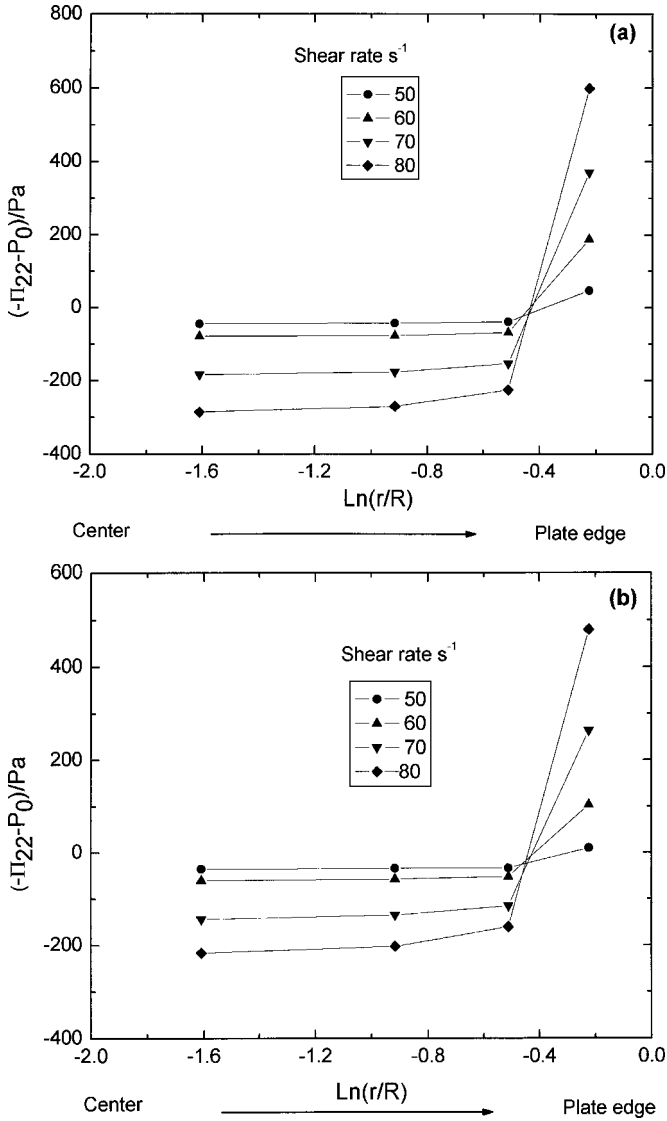


FIG. 9. Time-averaged radial pressure profiles measured for two different samples of the model colloidal dispersion during shear-rate-sweep experiments using parallel-plate fixtures at the rim shear rates given in the legend. The plate radius was 1.25 cm, and the gap between the plates was 0.86 mm in (a), and 0.89 mm in (b).

which is based on the assumption that Eq. (2) applies. For radial positions near the center of the plate, the local shear rate is probably below the critical value for onset of shear thickening. In this shear rate range, recall that the local pressure values were too small to measure in the cone-and-plate experiments. Hence, the measured pressure profile in the parallel plate rheometer is essentially flat in Fig. 9 at smaller radial positions. At the onset of shear thickening, the cone-and-plate measurements have shown that the normal stress differences increase sharply in magnitude (Fig. 4 and Table I). This probably explains the sharp break in the slope of the parallel-plate pressure profiles near the rim (Fig. 9), since all the terms in Eq. (2) depend on the normal stress differences. According to Eq. (2), the local slope of the pressure profiles in Fig. 9 $[-d\Pi_{22}/d(\ln r)]$ should equal $-N_1 - N_2$

$-\dot{\gamma}dN_2/d\dot{\gamma}$ at each radial position. The cone-and-plate measurements (Fig. 4 and Table I) have shown that the first term is negative but approaching zero at approximately 100 s^{-1} , and that the second and third terms are positive for shear rates above 60 s^{-1} with large magnitudes that increase strongly with increasing shear rate. Thus, near the rim at the highest rim shear rate value (80 s^{-1}), Eq. (2) in conjunction with cone-and-plate results predicts a positive slope for the parallel-plate pressure profile, as is observed. At lower shear rates, the prediction of Eq. (2) is uncertain because we were unable to measure the shear-rate-derivative of N_2 appearing in Eq. (2). Hence, there is no compelling evidence from the measured pressure profile that the flow of the colloidal dispersion in the parallel-plate rheometer does not have the expected velocity field.

V. CONCLUSIONS

We have investigated the behavior of all three steady shear flow properties (η , N_1 , N_2) for a model Brownian suspension of sterically stabilized PMMA colloids in DOP at a single particle size ($a=300 \text{ nm}$). The normal stress difference results presented here should be viewed as being complementary to previous experimental studies of suspensions of larger non-Brownian spheres at much high Peclet numbers [Zarraga *et al.* (2000); Singh and Nott (2003)]. The colloidal system of this work is thought to approximate a suspension of hard spheres with an added repulsive force of short range associated with the steric layer as in the two-particle model of Bergholtz *et al.* (2002). Therefore, it is reasonable to compare the experimental results presented here to the predictions of Stokesian dynamics simulations of smooth hard spheres [Foss and Brady (2000); Singh and Nott (2000)], as well as to the predicted rheological effects of small deviations from the hard sphere potential [Bergholtz *et al.* (2002)]. The simulations predict a viscosity shear-thickening transition, and this is observed experimentally, albeit at a higher critical Peclet number than predicted for smooth hard spheres, which is consistent with the presence of an additional short range repulsive force. At shear rates below the onset of shear thickening, N_1 was shown here to be positive though small in magnitude. At shear rates above the viscosity shear-thickening transition, N_1 was shown both here (Fig. 4) and in previous studies [Zarraga *et al.* (2000); Singh and Nott (2003)] to be negative. Hence, the simulation prediction [Foss and Brady (2000)] that N_1 changes sign from positive to negative has been verified experimentally, though the sign change occurs at a shear rate above the shear-thickening transition, possibly due once again to the presence of an extra repulsive force [Bergholtz *et al.* (2002)]. Above the onset of viscosity shear thickening, the pressure was found to increase with radial position r in both cone-and-plate and parallel-plate rheometers, even at shear rates for which N_1 was positive. This highly unusual behavior implies that the value of N_2 is negative and of large magnitude ($|N_2| > |N_1|$). This finding is also consistent with simulations [Sierou and Brady (2002); Singh and Nott (2000); Bergholtz *et al.* (2002)] and previous experimental studies at much higher Peclet numbers [Zarraga *et al.* (2000); Singh and Nott (2003)]. However, in previous colloidal experimental studies, the actual velocity field present in the rheometer has rarely if ever been measured, and nuclear magnetic resonance visualization studies have shown that the cone-and-plate velocity field can be anomalous for complex fluids [Britton and Callaghan (1997)]. The radial pressure profile measured here in the cone-and-plate rheometer does not obey the required functional form. Thus, at shear rates above the onset of viscosity shear thickening, the flow of the model colloid violates at least one of the assumptions expected to be valid for cone-and-plate shearing flows, possibly due to particle-jamming near the cone tip.

ACKNOWLEDGMENTS

Acknowledgment is made by two of the authors (M. L. and J. J. M.) to the Donors of the Petroleum Research Fund, administered by the American Chemical Society. One of the authors (M.A.) would like to acknowledge Stephen Hutcheson from the Department of Chemical Engineering at Texas Tech University for his help in performing the parallel-plate shearing flow experiments.

References

- Ackerson, B. J., and P. N. Pusey, "Shear-induced order in suspensions of hard spheres," *Phys. Rev. Lett.* **61**, 1033–1036 (1988).
- Adams, N., and A. S. Lodge, "A cone-and-plate and parallel-plate pressure distribution apparatus for determining normal stress differences in steady shear flow," *Philos. Trans. R. Soc. London, Ser. A* **A256**, 149–184 (1964).
- Antl, L., J. W. Goodwin, R. D. Hill, R. H. Ottewill, S. M. Owens, S. Papworth, and J. A. Waters, "The preparation of poly(methyl methacrylate) lattices in non-aqueous media," *Colloids Surf.* **17**, 67–78 (1986).
- Baek, S.-G., and J. J. Magda, "Monolithic rheometer plate fabricated using silicon micromachining technology and containing miniature pressure sensors for N_1 and N_2 measurement," *J. Rheol.* **47**, 1249–1260 (2003).
- Bender, J. A., and N. J. Wagner, "Reversible shear-thickening in monodisperse and bidisperse colloidal dispersions," *J. Rheol.* **40**, 899–916 (1996).
- Bergenholtz, J., J. F. Brady, and M. Vacic, "The non-Newtonian rheology of dilute colloidal suspensions," *J. Fluid Mech.* **456**, 239–275 (2002).
- Bird, R. B., R. C. Armstrong, and O. Hassager, *Dynamics of Polymeric Liquids*, 2nd Ed. (Wiley, New York, 1987), Vol. 1, pp. 521–524.
- Bossis, G., and J. F. Brady, "The rheology of Brownian suspensions," *J. Chem. Phys.* **91**, 1866–1874 (1989).
- Brady, J. F., and J. F. Morris, "Microstructure of strongly sheared suspensions and its impact on rheology and diffusion," *J. Fluid Mech.* **348**, 103–139 (1997).
- Brady, J. F., "Normal stresses in suspensions," in *Proc. of the XIIIth Int. Congress on Rheology*, Cambridge, UK, 2000, pp. I-34–I-37.
- Britton, M. M., and P. T. Callaghan, "Nuclear magnetic resonance visualization of anomalous flow in cone-and-plate rheometry," *J. Rheol.* **41**, 1365–1386 (1997).
- Campbell, A. I., and P. Bartlett, "Fluorescent hard-sphere polymer colloids for confocal microscopy," *J. Colloid Interface Sci.* **256**, 325–330 (2002).
- Chow, A. W., S. W. Sinton, J. H. Iwamiya, and T. S. Stephens, "Shear-induced particle migration in Couette and parallel-plate viscometers: NMR imaging and stress measurements," *Phys. Fluids* **6**, 2561–2576 (1994).
- D'Haene, P., J. Mewis, and G. G. Fuller, "Scattering dichroism measurements of flow-induced structure of a shear thickening suspension," *J. Colloid Interface Sci.* **156**, 350–358 (1993).
- de Kruijff, C. G., E. M. F. van Iersel, A. Vrij, and W. B. Russel, "Hard sphere colloidal dispersions: Viscosity as a function of shear rate and volume fraction," *J. Chem. Phys.* **83**, 4717–4725 (1985).
- Foss, D. R., and J. F. Brady, "Structure, diffusion and rheology of Brownian suspensions by Stokesian Dynamics simulation," *J. Fluid Mech.* **407**, 167–200 (2000).
- Frith, W. J., P. D'Haene, R. Buscall, and J. Mewis, "Shear thickening in model suspensions of sterically stabilized particles," *J. Rheol.* **40**, 531–548 (1996).
- Huilgol, R. R. and N. Phan-Thien, *Fluid Mechanics of Viscoelasticity* (Elsevier, New York, 1997), pp. 334–338.
- Hutcheson, S. A., X. F. Shi, and G. B. McKenna, "Performance comparison of a custom strain gauge based load cell with a rheometric series force rebalance transducer," *Proceedings of the Annual Technical Conference (ANTEC) of the Society of Plastics Engineers*, Chicago, IL, 16–20 May, 2004, pp. 2272–2276.
- Kolli, V. G., E. J. Pollauf, and F. Gadala-Maria, "Transient normal stress response in a concentrated suspension of spherical particles," *J. Rheol.* **46**, 321–334 (2002).
- Krishnamurthy, L.-K., N. J. Wagner, and J. Mewis, "Shear-thickening in polymer stabilized colloidal disper-

- sions," *J. Rheol.* **49**, 1347–1360 (2005).
- Larson, R. G., "Instabilities in viscoelastic flows," *Rheol. Acta* **31**, 213–263 (1992).
- Lee, C. S., B. C. Tripp, and J. J. Magda, "Does N_1 or N_2 control the onset of edge fracture?," *Rheol. Acta* **31**, 306–308 (1992).
- Lee, J.-D., J. H. So, and S. M. Yang, "Rheological behavior and stability of concentrated silica suspensions," *J. Rheol.* **43**, 1117–1140 (1999).
- Lee, M., M.S. thesis, University of Utah, Salt Lake City, UT (2004).
- Magda, J. J., S.-G. Baek, K. L. DeVries, and R. G. Larson, "Shear flows of liquid crystal polymers: Measurements of the second normal stress difference and the Doi molecular theory," *Macromolecules* **24**, 4460–4468 (1991).
- Magda, J. J., and S. G. Baek, "Concentrated entangled and semidilute entangled polystyrene solutions and the second normal stress difference," *Polymer* **35**, 1187–1194 (1994).
- Maranzano, B. J., and N. J. Wagner, "The effects of interparticle interactions and particle size on reversible shear thickening: Hard-sphere colloidal dispersions," *J. Rheol.* **45**, 1205–1222 (2001).
- Melrose, J. R., J. H. van Vliet, and R. C. Ball, "Continuous shear thickening and colloid surfaces," *Phys. Rev. Lett.* **77**, 4660 (1996).
- Mewis, J., W. J. Frith, T. A. Strivens, and W. B. Russel, "The rheology of suspensions containing polymerically stabilized particles," *AIChE J.* **35**, 415–499 (1989).
- Mewis, J., and G. Biebau, "Shear thickening in steady and superposition flows effect of particle interaction forces," *J. Rheol.* **45**, 799–813 (2001).
- Narumi, T., H. See, Y. Honma, T. Hasegawa, T. Takahashi, and N. Phan-Thien, "Transient response of concentrated suspensions after shear reversal," *J. Rheol.* **46**, 295–305 (2002).
- Niemiec, J. M., J.-J. Pesce, and G. B. McKenna, "Anomalies in the normal force measurement when using a force rebalance transducer," *J. Rheol.* **40**, 323–334 (1996).
- Pathmamanoharan, C., K. Groot, and J. K. G. Dhont, "Preparation and characterization of crosslinked PMMA latex particles stabilized by grafted copolymer," *Colloid Polym. Sci.* **275**, 897–901 (1997).
- Petekidis, G., A. Moussaid, and P. N. Pusey, "Rearrangements in hard-sphere glasses under oscillatory shear strain," *Phys. Rev. E* **66**, 051402 (2002).
- Petekidis, G., D. Vlassopoulos, and P. N. Pusey, "Yielding and flow of sheared colloidal glasses," *J. Phys.: Condens. Matter* **16**, S3955–S3963 (2004).
- Phung, T. N., J. F. Brady, and G. Bossis, "Stokesian dynamics simulation of Brownian suspensions," *J. Fluid Mech.* **313**, 181–207 (1996).
- Rampall, I., J. R. Smart, and D. T. Leighton, "The influence of surface roughness on the particle-pair distribution function of dilute suspensions of noncolloidal spheres in simple shear flow," *J. Fluid Mech.* **339**, 1–24 (1997).
- Royall, C. P., M. E. Leunissen, and A. van Blaaderen, "A new colloidal model system to study long-range interactions quantitatively in real space," *J. Phys.: Condens. Matter* **15**, S3589–S3596 (2003).
- Russel, W. B., D. A. Saville, and W. R. Schowalter, *Colloidal Dispersions* (Cambridge University Press, London, 1989).
- Sierou, A., and J. F. Brady, "Rheology and microstructure in concentrated noncolloidal suspensions," *J. Rheol.* **46**, 1031–1056 (2002).
- Singh, A., and R. Nott, "Normal stresses and microstructure in bounded sheared suspension via Stokesian dynamics simulations," *J. Fluid Mech.* **412**, 279–301 (2000).
- Singh, A., and P. R. Nott, "Experimental measurements of the normal stresses in sheared Stokesian suspensions," *J. Fluid Mech.* **490**, 293–320 (2003).
- Tanner, R. I., and M. Keentok, "Shear fracture in cone-plate rheometry," *J. Rheol.* **27**, 47–57 (1983).
- Turian, R. M., "Perturbation solution of the steady Newtonian flow in the cone and plate and parallel-plate systems," *Ind. Eng. Chem. Fundam.* **11**, 361–368 (1972).
- Yethiraj, A., and A. van Blaaderen, "A colloidal model system with an interaction tunable from hard sphere to soft and dipolar," *Nature (London)* **421**, 513–517 (2003).
- Zarraga, I. E., D. A. Hill, and D. T. Leighton, "The characterization of the total stress of concentrated suspensions of noncolloidal spheres in Newtonian fluids," *J. Rheol.* **44**, 185–220 (2000).